4172–4180 *Nucleic Acids Research, 2008, Vol. 36, No. 12* *Published online 16 June 2008*
doi:10.1093/nar/gkn360

Studies on *Methanocaldococcus jannaschii* RNase P reveal insights into the roles of RNA and protein cofactors in RNase P catalysis

Dileep K. Pulukkunat and Venkat Gopalan*

Ohio State Biochemistry Program and Department of Biochemistry, The Ohio State University, Columbus, OH 43210, USA

Received April 20, 2008; Revised May 15, 2008; Accepted May 20, 2008

ABSTRACT

Ribonuclease P (RNase P), a ribonucleoprotein (RNP) complex required for tRNA maturation, comprises one essential RNA (RPR) and protein subunits (RPPs) numbering one in bacteria, and at least four in archaea and nine in eukarya. While the bacterial RPR is catalytically active *in vitro*, only select euryarchaeal and eukaryal RPRs are weakly active despite secondary structure similarity and conservation of nucleotide identity in their putative catalytic core. Such a decreased archaeal/eukaryal RPR function might imply that their cognate RPPs provide the functional groups that make up the active site. However, substrate-binding defects might mask the ability of some of these RPRs, such as that from the archaeon *Methanocaldococcus jannaschii* (*Mja*), to catalyze precursor tRNA (ptRNA) processing. To test this hypothesis, we constructed a ptRNA-*Mja* RPR conjugate and found that indeed it self-cleaves efficiently (k_{obs}, 0.15 min^{-1} at pH 5.5 and 55°C). Moreover, one pair of *Mja* RPPs (POP5-RPP30) enhanced k_{obs} for the RPR-catalyzed self-processing by ~100-fold while the other pair (RPP21-RPP29) had no effect; both binary RPP complexes significantly reduced the monovalent and divalent ionic requirement. Our results suggest a common RNA-mediated catalytic mechanism in all RNase P and help uncover parallels in RNase P catalysis hidden by plurality in its subunit make-up.

INTRODUCTION

Ribonuclease P (RNase P) is an endoribonuclease responsible for the 5′ maturation of tRNAs. It is a ribonucleoprotein (RNP) complex containing one essential RNA (RNase P RNA; RPR) in all three domains of life and a varying number of protein subunits (RNase P Protein; RPP): one in bacteria, and at least four and nine in archaea and eukarya, respectively (1–6). The bacterial RPR is catalytically active in the absence of its RPP under *in vitro* conditions that include a high concentration of Mg^{2+} (or another suitable divalent metal ion) which is essential for catalysis (1). However, only a few representative archaeal and eukaryal RPRs are weakly active under various conditions tested *in vitro* (6–9). This result is surprising given the remarkable secondary structure similarity and conservation of nucleotide identity in the putative catalytic core in all RPRs and raises the possibility that not all RPRs are functionally equivalent (Figure 1A–C; 10). We investigate here a euryarchaeal RPR that was reported to be inactive when tested alone (7,8) and examine the basis for its inactivity and its cooperation with cognate RPPs during catalysis.

Based on the conserved structural elements of the RPR, euryarchaeal RNase P is classified into types A and M (8). At the secondary structure level, type A RPRs resemble the ancestral bacterial RPRs while type M RPRs lack some of the structural elements implicated in substrate binding in bacterial RPRs (Figure 1A–C; 8,10,11). Consistent with this observation, only a few type A RPRs and none of the type M RPRs are catalytically active *in vitro* without their RPPs (7). In this study, we employ *Methanocaldococcus jannaschii* (*Mja*) RPR as a prototype for type M RPRs. Using a unimolecular enzyme-substrate conjugate expected to alleviate substrate-binding defects in *Mja* RPR, we establish that *Mja* RPR (in the absence of RPPs) supports cleavage in cis, thus reaffirming the RPR's pivotal catalytic role.

If the RPR is the catalytic moiety in RNase P from all three domains of life, why do archaeal/eukaryal RNase P holoenzymes require multiple RPPs for function *in vivo* while bacterial RNase P employs a single RPP, which serves to normalize the binding affinity and rate of cleavage of different precursor tRNAs (ptRNAs) by the RPR (12–15)? Biochemical characterization of a partially purified archaeal RNase P holoenzyme demonstrated that the RPR is associated with at least four RPPs (POP5, RPP30,

*To whom correspondence should be addressed. Tel: +614 292 1332; Fax: +614 292 6773; Email: gopalan.5@osu.edu

RPP21 and RPP29), which have eukaryal homologs (2,3). We recently reconstituted *Pyrococcus furiosus* (*Pfu*; type A) RNase P *in vitro* in an effort to develop archaeal RNase P as an experimental surrogate for the more complex eukaryal counterpart (16). In this study, by examining the role of RPPs in aiding the self-processing of the type M RPR-ptRNA cis conjugate, we are beginning to uncover functional parallels between the archaeal RPPs and the sole bacterial RPP.

MATERIALS AND METHODS

Cloning of RPRs and ptRNA-RPR cis conjugates

Complete details are provided in the Supplementary Data.

RNase P activity assays

The hybrid RPR and cis conjugates were folded as follows: incubation at 50°C for 50 min in water followed by 37°C for 30 min in 50 mM Tris-acetate (pH 8) containing either 100 mM $Mg(OAc)_2$ and 2.5 M NH_4OAc (for pt^{Tyr}-S_5-M RPR) or 10 mM $Mg(OAc)_2$ and 800 mM NH_4OAc (for pt^{Tyr}-S_3-M, pt^{Tyr}-S_3-ΔS M and *Eco*S-*Mja*C RPRs).

In the absence of RPPs, trans cleavage by the hybrid RPR or self-cleavage by the cis conjugates was initiated by addition of 500 mM $Mg(OAc)_2$ (or the amounts indicated if the experiment was a titration analysis).

To ensure that pt^{Tyr}-S_3-M RPR does not self-cleave during reconstitution with *Mja* RPPs, we used two different pre-incubation strategies that permit assembly without promoting significant cleavage (Table 1). In the first approach, 50 nM pt^{Tyr}-S_3-M RPR was mixed with 250 nM of each binary complex in 50 mM MES (pH 5.1 at 55°C), 800 mM NH_4OAc, and either 1 mM $Mg(OAc)_2$ (for POP5-RPP30) or 10 mM $Mg(OAc)_2$ (for RPP21-RPP29). In the second approach, which was necessary for the reaction performed in the presence of all four RPPs, 25 mM Ca^{2+} replaced Mg^{2+} in the pre-incubation step. In both instances, reactions were initiated by adding an equal volume of 50 mM MES (pH 5.1 at 55°C), 800 mM NH_4OAc, and 200 mM $Mg(OAc)_2$ (final $[Mg^{2+}]$ = 100 mM).

Unless stated otherwise, all assays involved incubation for a specified period at 55°C in a thermal cycler. Reactions were terminated by adding an equal volume of stop solution [10 M urea, 5 mM EDTA, 0.05% (w/v) xylene cyanol, 10% (v/v) phenol]; if the time of incubation was short (e.g. 5 s) to accommodate rapid cleavage, reactions were terminated by first immersing the reaction tubes in liquid nitrogen and subsequently adding stop solution.

Kinetic analysis

The substrate and product RNAs were separated on either 8% or 10% (w/v) polyacrylamide/7 M urea gels and visualized by PhosphorImaging (Molecular Dynamics). The extent of cleavage was quantitated using ImageQuant (Molecular Dynamics) software. To obtain the rate of product formation (k_{obs}), the % product formed at time t (P_t) was fit to $P_t = P_\infty(1 - e^{-kt})$ using Kaleidagraph software (Synergy). Background cleavage during the 20-min pre-incubation used for RNP assembly was typically less than 5% and corrected using $P_t = P_o + (P_\infty - P_o)(1 - e^{-kt})$, where P_o refers to product formed at t_o (i.e. the end of the pre-incubation). In the cis conjugate reactions, the maximum product formed varied from 25 to 95% depending on the catalytic entity tested and assay pH.

Dependence of rate on assay pH

The rate of product formation was determined at 55°C and various pH values: 5.1–6.3 for pt^{Tyr}-S_3-M RPR, 4.65–5.1 for pt^{Tyr}-S_3-M RPR + POP5-RPP30, and 5.4–7.1 for pt^{Tyr}-S_3-ΔS M RPR; 50 mM ammonium acetate (pH<5) or MES (pH>5) or HEPES (>6.5) buffers were employed in these assays. At each pH, at least three replicates were performed to obtain the mean and standard deviation values.

RESULTS

Archaeal type M RPR supports ptRNA processing independently of its cognate RPPs

Under prolonged incubation at pH 6 in the presence of 0.2 M Mg^{2+} and 0.8 M NH_4^+, human RPR was recently demonstrated to process a ptRNA-based model substrate (k_{obs} ~10^{-5} min^{-1}, the pseudo-first order rate constant under single-turnover conditions; 9). Subsequently, the *Cyanophora paradoxa* cyanelle RPR, which is part of an RNase P with high protein content, was also reported to exhibit ptRNA cleavage at pH 6, 0.1 M Mg^{2+} and 0.1M NH_4^+ (k_{obs} ~ 10^{-3} min^{-1}; 17). However, when we examined if the euryarchaeal type M RPRs would be active under analogous assay conditions with *Escherichia coli* (*Eco*) $ptRNA^{Tyr}$ as the substrate, we observed no activity with the *Archaeoglobus fulgidus* (*Afu*) and *Mja* RPRs (data not shown). No ptRNA processing activity was evident even with a variety of other assay conditions tested (37–55°C; 0.1–0.4 M Mg^{2+}, 0.8–3 M NH_4^+, pH 6–7.5; and RPR concentrations up to 20 μM; data not shown). The failure of type M RPRs to catalyze ptRNA cleavage in trans contrasts with the human RPR and might reflect differences in their structures.

If the inability of *Afu* and *Mja* RPRs to catalyze ptRNA processing is due to the absence of specific RNA structural elements (e.g. P8, L15; Figure 1C) implicated in ptRNA binding in the bacterial RPR (Figure 1A; 8,11,18–21), alleviation of substrate-binding defects might render the type M RPR active. Towards this objective, we constructed a bacterial-archaeal (type M) hybrid RPR based on three observations. First, biochemical studies delineated the presence of two independently folding modules in bacterial RPRs: a substrate-specificity (S) domain that has conserved nucleotides for recognition of the T stem-loop of the ptRNA; and a catalytic (C) domain which can (i) recognize the leader, acceptor stem, and the 3′ terminal CCA sequence, and (ii) cleave the ptRNA (18–24). Second, we recently demonstrated that in *Pfu* RPR (euryarchaeal type A), the C domain was capable of cleaving ptRNA in the presence of two of its cognate RPPs (16). Lastly, mitochondrion-encoded RPRs in jakobid flagellates (e.g. *Reclinomonas americana*) became active upon

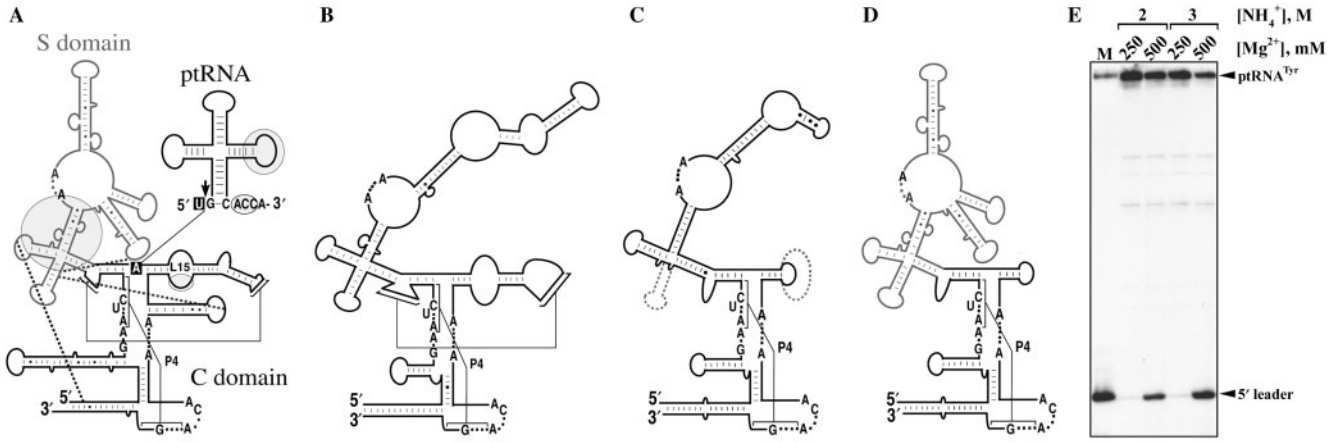

Figure 1. An RPR hybrid comprising an S and C domain from a bacterial and an archaeal type M RPR, respectively, is catalytically active and can accurately process ptRNA^{Tyr}. (**A**) The shaded circles, ovals, and black boxes depict known interactions between the *Eco* RPR and a ptRNA substrate (11). Arrow indicates the site of cleavage in the ptRNA. In the RPR, the C and S domains are indicated in black and gray, respectively. Thick dotted lines indicate tertiary interactions unique to the bacterial RPR. (**B** and **C**) Secondary structures of representative archaeal type A and M RPRs, respectively. The structural elements absent in type M RPR (C) are highlighted with dotted lines. (**D**) Secondary structure of the bacterial/archaeal hybrid RPR (*Eco*S-*Mja*C RPR) used in this study. The S domain of bacterial RPR is indicated in gray. Universally conserved nucleotides are indicated in A–D. (**E**) *Eco*S-*Mja*C RPR (2.5 μM) was tested for RNase P activity by incubating at 50°C for 15 min with 5′ labeled ptRNA^{Tyr} (~1 pM) in 50 mM Tris-acetate (pH 8) and different NH_4^+ and Mg^{2+} concentrations as indicated. M represents a size marker generated by processing of ptRNA^{Tyr} by *Eco* RNase P.

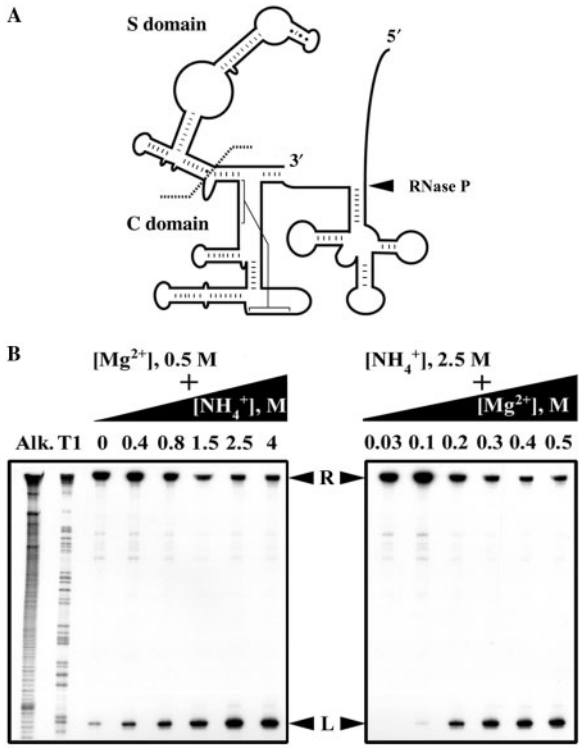

Figure 2. Design and optimization of self-cleavage conditions for an active-site tethered ES conjugate. (**A**) Illustration of pt^{Tyr}-S_3 (and S_5)-M RPR in which ptRNA^{Tyr} is attached to L15 of *Mja* RPR with either a 3- or 5-nt spacer. The C and S domains are demarcated to indicate what was deleted in pt^{Tyr}-S_3-ΔS M RPR. (**B**) Titration of monovalent and divalent cations to identify the optimal conditions for maximal self-cleavage of 5′ labeled pt^{Tyr}-S_5-M RPR (see text for details). R and L indicate RPR cis conjugate and the 5′ leader, respectively.

fusion of their C domains with the S domain of *Eco* RPR (25). Therefore, guided in part by the recent high-resolution structures of bacterial RPRs (26,27) and prior biochemical studies in which similar hybrids were generated, we constructed a hybrid RPR with the S domain of *Eco* RPR fused to the putative C domain of *Mja* RPR (*Eco*S-*Mja*C RPR; Figure 1D and Supplementary Data). Indeed, *Eco*S-*Mja*C RPR accurately processes ptRNA^{Tyr} (Figure 1E). Therefore, *Mja* RPR supports trans cleavage of ptRNA^{Tyr} if its S domain, probably defective in substrate binding, is replaced with a bacterial S domain that does not suffer from this limitation.

Since the above experiment revealed that the *Mja* RPR's inactivity is likely due to defects in ptRNA recognition/binding, we inquired if an enzyme-substrate (ES) covalent conjugate in which a ptRNA is covalently tethered to the *Mja* RPR would facilitate its processing. However, we did not observe any cis cleavage when we tested conjugates in which ptRNA^{Tyr} was attached to the 3′ end of either *Afu* or *Mja* RPR [with spacers of either 50 nts (*Afu*) or 25 nts (*Mja*) to the cleavage site; data not shown].

As there was precedence for bacterial and archaeal type A RPRs supporting cis cleavage of a ptRNA attached to the L15 loop (7,28), we made similar constructs with *Mja* RPR especially since L15 is likely to be part of the active site in bacterial RPR (Figure 2A; see Supplementary Data; 20,21,26,27). When we tested such conjugates with spacers of 0, 5 and 10 nts, only the latter two were cleaved. However, since the 10-nt-spacer conjugate also exhibited some mis-cleavage, only the 5-nt-spacer conjugate was characterized further. The accuracy of cleavage in ptRNA^{Tyr}-S_5-*Mja* RPR (abbreviated as pt^{Tyr}-S_5-M RPR; Figure 2A) was confirmed by comparing the migration of the 5′ leader with that of a size marker generated by partial digestion of 5′ labeled pt^{Tyr}-S_5-M RPR with RNase T1 (Figure 2B).

To identify conditions that permit efficient and accurate self-cleavage of pt^{Tyr}-S_5-M RPR, we varied different parameters. Either the Mg^{2+} concentration was held constant

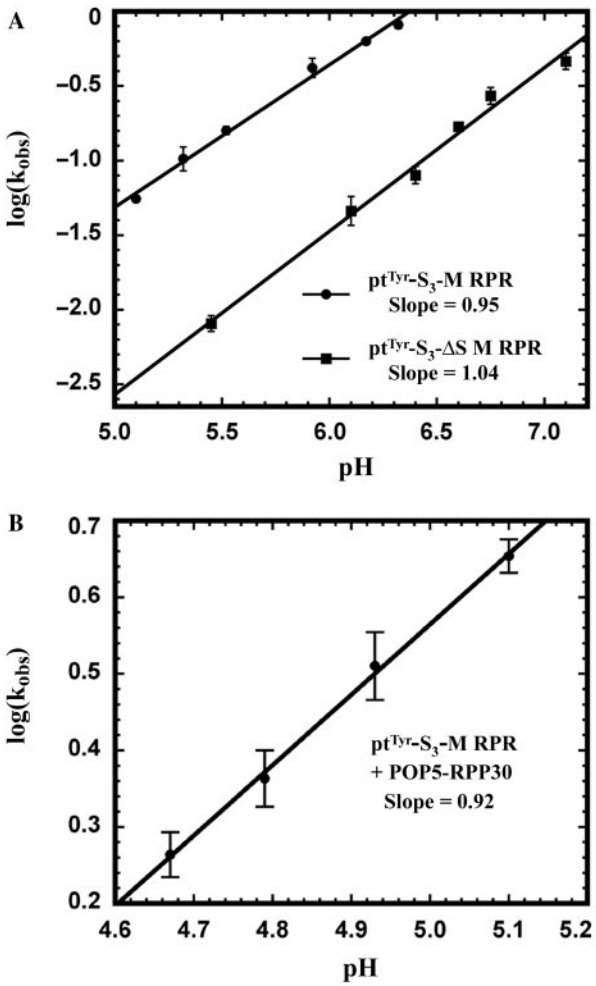

Figure 3. Dependence of k_{obs} on assay pH for self-cleavage of pt^{Tyr}-S_3-M RPR and pt^{Tyr}-S_3-ΔS M RPR (**A**) and pt^{Tyr}-S_3-M RPR + POP5-RPP30 (**B**).

at 0.5 M while the NH_4^+ concentration was increased from 0 to 4 M, or the NH_4^+ concentration was maintained at 2.5 M while the Mg^{2+} concentration was raised from 0 to 0.5 M (Figure 2B). Such experiments together with others where the assay pH or temperature was altered, established the optimal condition as 55°C in 50 mM Tris-acetate (pH 8), 500 mM $Mg(OAc)_2$ and 2.5 M NH_4OAc.

The extent of processing of 5′ labeled pt^{Tyr}-S_5-M RPR was determined by quantitating formation of the 5′ leader. A single exponential function adequately describes the rate of product formation (data not shown). We next inquired if the phosphodiester bond-breaking step is rate limiting. Deprotonation of a hydrated Mg^{2+} ion in the RPR's active site is believed to generate the hydroxide nucleophile for attacking the scissile phosphodiester linkage in the ptRNA substrate (29,30). Therefore, evidence for the chemical step being rate limiting is generally derived from correlating the rate of product formation with the hydroxide ion concentration (i.e. specific base catalysis; 30). A slope of ~1 in plots of $\log(k_{obs})$ versus pH reflects cleavage being the sole rate-limiting determinant; absence or decrease in such a dependence typically implies that other factors (e.g. conformational rearrangements, substrate docking) also contribute to the rate-limiting step.

When we assayed pt^{Tyr}-S_5-M RPR at pH 5.5 and 7.5, we observed only a 2-fold increase in k_{obs} as opposed to the 100-fold enhancement expected if the bond-breaking step is solely rate limiting. Based on the premise that there might be slower steps preceding the chemical step during self-cleavage of pt^{Tyr}-S_5-M RPR, we inquired if alterations in the length of the spacer (3, 4, 8 or 9 nts) might yield a cis conjugate whose rate is determined only by phosphodiester hydrolysis. Indeed, $\log(k_{obs})$ versus pH for the self-cleavage of a 3-nt-spacer conjugate, pt^{Tyr}-S_3-M RPR, exhibited a slope of 0.95 in the pH range 5.1–6.3 (Figure 3A). As expected for a first-order reaction, we found that the k_{obs} values at various pt^{Tyr}-S_3-M RPR concentrations are nearly identical.

The k_{obs} value of 0.15 min^{-1} at pH 5.5 and 55°C for pt^{Tyr}-S_3-M RPR compares favorably to 0.75 min^{-1} at pH 5.5 and 50°C reported for pt^{Asp}-S_5-*Eco* RPR (31). This parallel in k_{obs} values is striking given that the type M RPR lacks the functional S domain present in *Eco* RPR. Tethering of the substrate to the type M RPR appears to have rendered the S domain less essential. Importantly, the similar k_{obs} values, despite the different ptRNA substrates, sites of conjugation, and assay temperatures used in the two studies, might reflect comparable ptRNA cleavage potential for the C domains of bacterial and archaeal RPRs.

Only a subset of *Mja* RPPs influences the k_{obs} of pt^{Tyr}-S_3-M RPR self-cleavage

To examine the contribution of *Mja* RPPs to pt^{Tyr}-S_3-M RPR catalysis, we cloned the genes encoding *Mja* POP5, RPP21, RPP29 and RPP30 into vectors that allow T7 RNA polymerase-based overexpression in *E. coli* BL21(DE3) cells. Our previous studies on *in vitro* reconstituted *Pfu* RNase P revealed that the four RPPs function as two binary complexes (POP5-RPP30 and RPP21-RPP29; 16); therefore, we co-overexpressed the *Mja* RPPs as binary complexes in *E. coli*. By exploiting the high pI values of *Mja* RPPs (see Supplementary Data), we were able to purify the complexes to near homogeneity by cation-exchange chromatography. Details of the cloning, overexpression and purification of *Mja* RPPs will be described elsewhere. Purified *Mja* RPPs when combined with the *Mja* RPR generated a functional *Mja* RNase P holoenzyme that exhibited multiple turnover (k_{cat} ~ 6–24 min^{-1}) at 55°C with *Eco* $ptRNA^{Tyr}$ or *Synechocystis* $ptRNA^{Gln}$ (32) as the substrate. A k_{cat} value of 34 min^{-1} was reported for cleavage of *Bacillus subtilis* $ptRNA^{Asp}$ at 50°C by partially purified native *Mja* RNase P (33).

Both *Mja* POP5-RPP30 and RPP21-RPP29 decrease the concentration of monovalent and divalent ions required for cis cleavage of pt^{Tyr}-S_3-M RPR; the Mg^{2+} requirement decreases from 500 to 100 mM with either binary complex and decreases further to 20 mM with both (Figure 4A; Table 1). In addition, *Mja* POP5-RPP30, but not RPP21-RPP29, enhances by 100-fold the maximal k_{obs} for self-processing of pt^{Tyr}-S_3-M RPR at pH 5.1 and 55°C (0.05 to 4.8 min^{-1}; Table 1). A plot of log

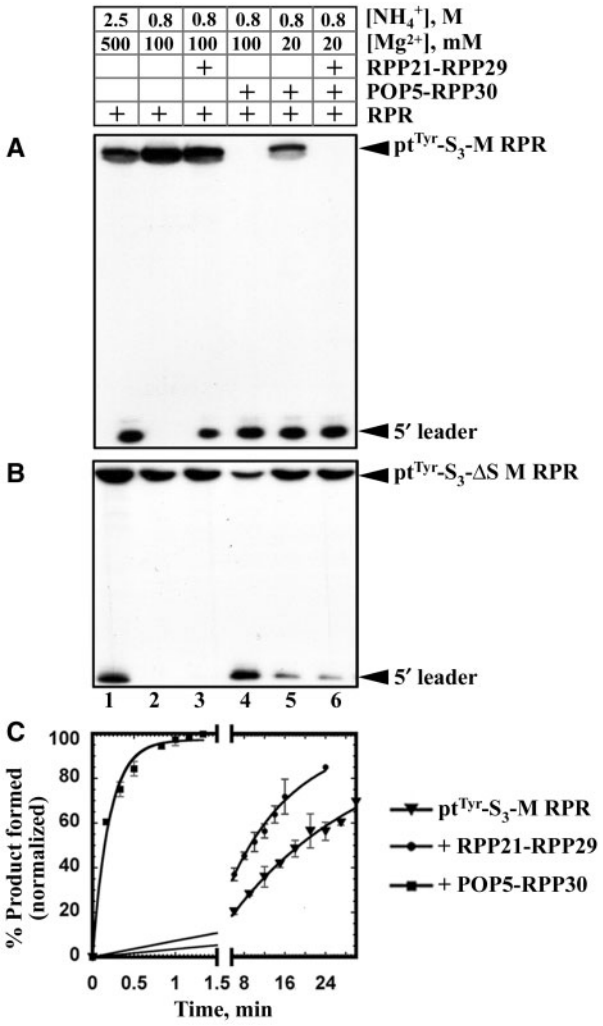

Figure 4. Effect of *Mja* RPPs on the self-processing rate of pt^{Tyr}-S_3-M RPR and pt^{Tyr}-S_3-ΔS M RPR. All assays were performed in 50 mM MES (pH 5.1) at 55°C. 5′ labeled pt^{Tyr}-S_3-M RPR (**A**) or pt^{Tyr}-S_3-ΔS M RPR (**B**) was reconstituted with binary complexes of *Mja* RPPs at various concentrations of monovalent and divalent cations as indicated. (**C**) Rate of self-cleavage of the pt^{Tyr}-S_3-M RPR without RPPs (triangles), with RPP21-RPP29 (circles) or with POP5-RPP30 (squares); assay conditions are listed in Table 1.

Table 1. Effect of *Mja* RPPs on the ionic requirements and rate of self-processing of pt^{Tyr}-S_3-M and pt^{Tyr}-S_3-ΔS M RPR conjugates at pH 5.1 and 55°C

RNase P assayed	k_{obs}, min^{-1}	$[NH_4^+]$, M	$[Mg^{2+}]$, M
Reconstituted and pre-incubated with low $[Mg^{2+}]$			
pt^{Tyr}-S_3-M RPR	0.05 ± 0.01	2.5	0.5
+ RPP21-RPP29	0.06 ± 0.01	0.8	0.1
+ POP5-RPP30	4.83 ± 0.02	0.8	0.1
Reconstituted and pre-incubated with Ca^{2+}			
pt^{Tyr}-S_3-M RPR			
+ POP5-RPP30	5.16 ± 0.08	0.8	0.1
+ 4 RPPs	5.46 ± 0.04	0.8	0.1
pt^{Tyr}-S_3-ΔS M RPR*	0.004*	2.5	0.5
+ POP5-RPP30	4.86 ± 0.06	0.8	0.1

*Rate at pH 5.1 obtained by extrapolating from values obtained between pH 5.4 and 7.1 (Fig. 3A).

(k_{obs}) versus pH for the pt^{Tyr}-S_3-M RPR + POP5-RPP30 exhibited a slope of 0.92 (Figure 3B). Slopes close to unity in plots of log(k_{obs}) versus pH for the self-cleavage of pt^{Tyr}-S_3-M RPR with and without POP5-RPP30 indicate that the chemical step is rate limiting in both instances.

We next determined whether all four RPPs together will enhance k_{obs} to a level greater than that observed with just POP5-RPP30. However, technical issues prevented us from doing this experiment under conditions employed for the binary complexes. For reactions involving the RPR reconstituted with RPPs, we typically employ a pre-incubation step (10 min at 37°C followed by 10 min at 55°C) in a Mg^{2+}-containing buffer to permit RNP assembly prior to substrate addition (16). Since such an approach with the cis conjugate and four RPPs triggers significant self-cleavage during the pre-incubation step, we devised an alternative strategy.

As kinetic and thermodynamic studies using bacterial RPRs and ptRNAs revealed that the RPR adopts the correct tertiary fold for optimal ES complex formation with Ca^{2+}, a divalent cation that promotes efficient ptRNA binding but not processing (30), we pre-incubated pt^{Tyr}-S_3-M RPR either with all four RPPs or just POP5-RPP30 in a buffer containing 25 mM Ca^{2+} instead of Mg^{2+}; cleavage was then initiated by adding an excess of Mg^{2+} to displace the Ca^{2+}. To estimate the concentration of Mg^{2+} required for displacing the Ca^{2+} and promoting maximal cleavage, the rate of self-processing was determined with a Mg^{2+}-titration analysis from 10 to 150 mM Mg^{2+}, which revealed that 100 mM Mg^{2+} is optimal.

Despite the viability of the above approach, it is conceivable that the calculated rate is influenced adversely by the pre-incubation with Ca^{2+} and its subsequent displacement by Mg^{2+}. Therefore, we compared the k_{obs} for self-processing of pt^{Tyr}-S_3-M RPR + POP5-RPP30 under two conditions: assembled in a pre-incubation buffer containing either 1 mM Mg^{2+} or 25 mM Ca^{2+} and subsequently assayed in the presence of 100 mM Mg^{2+}. In both cases, the result was similar (4.8 versus 5.2 min^{-1}), thus validating the Ca^{2+}-based approach. Using this method, we determined that the k_{obs} for pt^{Tyr}-S_3-M RPR self-cleavage with just POP5-RPP30 (5.2 min^{-1}) was not appreciably enhanced by addition of RPP21-RPP29 (5.5 min^{-1}; Table 1).

In the studies described above, due to technical issues thwarting the use of a rapid quench flow apparatus to perform transient kinetic assays at near-neutral pH and 55°C, we used an assay pH of 5.1 to enable manual determination for the rate of self-cleavage of pt^{Tyr}-S_3-M RPR. Such an approach might be subject to the limitation that protein–protein interactions at pH 5.1 might differ from those occurring at physiological pH.

Removal of the S domain from pt^{Tyr}-S_3-M RPR does not eliminate self-cleavage activity

Deletion mutagenesis studies on type A bacterial (e.g. *Eco*) and archaeal (e.g. *Pfu*) RPRs established that their C domains support catalysis albeit only in the presence of cognate RPPs (16,22,23,34). With the C domain of *B. subtilis* RPR (bacterial type B), the cleavage rate was

25 000-fold lower compared to the wild-type RPR and 40-fold lower in the presence of the RPP (35). These observations, together with results from footprinting and kinetic studies (18,19), suggest that the S domain contributes to ptRNA recognition and helps position the substrate for optimal cleavage. Reasoning that the decreased efficiency of ptRNA processing with the C domains of bacterial/archaeal RPRs is likely due to substrate-binding/positioning defects caused by removal of the S domain, we hypothesized that the *Mja* RPR-ptRNA cis conjugate should be active even without the S domain since the substrate is covalently tethered to the enzyme. Indeed, pt^{Tyr}-S_3-ΔS M RPR, the cis conjugate lacking the S domain, is active (Figure 4B, lane 1). Interestingly, instead of the 25 000-fold defect observed in the trans cleavage scenario with the C domain of *B. subtilis* RPR (35), cleavage of pt^{Tyr}-S_3-ΔS M RPR is only 12-fold slower than pt^{Tyr}-S_3-M RPR at pH 5.1 (0.004 versus $0.05\,min^{-1}$; Figure 3A; Table 1). Clearly, removal of the S domain has a more adverse impact on the trans compared to the cis cleavage reaction used here. The activity of the ΔS M RPR also attests to the ptRNA processing ability of the C domains of all RPRs, even those bereft of the functionally important L15 and the neighboring P16/P17 helices present in the bacterial RPR (9). The *Mja* ΔS RPR in pt^{Tyr}-S_3-ΔS M RPR also represents the smallest functional RPR yet identified (135 nts) and could be used in high-resolution structural studies.

We examined the effect of RPPs on the self-cleavage rate of pt^{Tyr}-S_3-ΔS M RPR. Addition of POP5-RPP30 resulted in a k_{obs} value of $4.9\,min^{-1}$, similar to $5.2\,min^{-1}$ observed with the wild type and indicates that this binary complex can compensate for the missing S domain. In contrast, addition of RPP21-RPP29 to pt^{Tyr}-S_3-ΔS M RPR impacts neither the rate nor the ionic requirement. This finding suggests that RPP21-RPP29 asserts its effect on the RPR by binding to the S domain, a claim confirmed by our ongoing footprinting analysis which indicates that RPP21-RPP29 binds to the S domain (unpublished observations).

DISCUSSION

RPR is the catalytic subunit of RNase P in all three domains of life

Although the bacterial RPR alone is catalytically active under *in vitro* conditions of high ionic strength, until recently RPRs from many archaeal and all eukaryal sources were reported as incapable of catalysis without their cognate RPPs. These archaeal and eukaryal RPRs were not rendered active even in the presence of high concentrations of monovalent and divalent cations, which occasionally mitigate structural defects that prevent generation of an active RNA tertiary fold (6–8,36,37). The decreased activity in these RPRs might reflect a natural course towards a more complex RNP in which protein subunits provide functional groups that make up the active site. However, results from a recent study and the data reported here do not support such a premise. First, Kikovska *et al.* (9) showed that the human RPR can process different ptRNAs and model substrates, albeit 10^6-fold slower than that of bacterial RPR. Second, we have demonstrated here through engineering strategies intended to overcome substrate-binding defects that a euryarchaeal type M RPR, thus far found to be incapable of ptRNA processing, can catalyze this reaction (Figures 1 and 2).

Since the human and *Mja* (archaeal type M) RPRs can support ptRNA processing in the absence of RPPs when 150–500 mM Mg^{2+} is provided, it is evident that they possess the crucial structural elements required for generating the active site. These findings together with the fact that all characterized RPPs, either individually or in combination, cannot promote ptRNA processing without their RPRs confirm that the RPR is the catalytic moiety in all three domains of life. While such a broad inference might seem inconsistent with reports of failure to detect archaeal/eukaryal RPR-alone-catalyzed ptRNA processing, these results might reflect either an inability to form an active RPR fold *in vitro* or a masking of the cleavage capability due to extremely weak ptRNA binding (37).

Cleavage by *Mja* RPR is significantly enhanced by POP5-RPP30 at lower Mg^{2+} concentrations

Addition of the sole bacterial RPP normalizes the binding affinity and rate of cleavage of different ptRNAs by the cognate RPR; moreover, it enhances the affinity for Mg^{2+} ions in the active site thereby making a vital contribution to rate enhancement at physiological Mg^{2+} concentrations (14,15). What then are the roles played by the multiple archaeal/eukaryal RPPs?

Our studies on *Pfu* RNase P, where we examined the trans cleavage of a ptRNA under multiple turnover conditions, revealed that POP5-RPP30 (but not RPP21-RPP29) enhances the k_{cat} of the RPR by nearly 40-fold, in fact to the same extent observed with all four RPPs (16). This finding indicated that POP5-RPP30 plays a vital role in cleavage and/or product release. Although a comprehensive description of the kinetic scheme requires determining the rate constants for individual steps, we rationalized that studying the *Mja* RPR cis conjugate in the absence and presence of its cognate RPPs might permit us to focus on the chemical step (akin to a single-turnover reaction) without influence from substrate binding or product release. Even for a cis conjugate, however, k_{obs} (the apparent rate of product formation) need not be the rate of the chemical step as steps prior to cleavage could be rate limiting (see scheme below).

The maximal k_{obs} for self-cleavage of pt^{Tyr}-S_3-M RPR is accelerated ~100-fold by *Mja* POP5-RPP30 but not at all by RPP21-RPP29 (Table 1). Similarly, only POP5-RPP30 promotes the trans cleavage of ptRNA by *Mja* RPR under multiple turnover conditions (unpublished observations). These findings are also consistent with our earlier observation that *Pfu* RPP21-RPP29 leaves the k_{cat} of the *Pfu* RPR-catalyzed reaction unaltered while decreasing the K_m five-fold and lowering the Mg^{2+} requirement (16).

We interpret our current results within a framework based on the kinetic scheme put forth by Harris and coworkers for trans cleavage of ptRNAs by *Eco* RNase

P (14). When the role of the *Eco* RPP in RPR-mediated cleavage of ptRNAs with and without consensus recognition sequences was examined in single-turnover reactions, the RPP increased by 100- to 1000-fold the k_{obs} for non-consensus ptRNA processing by the cognate RPR. The scheme below was used to explain the role of the bacterial RPP in catalysis. Subsequent to substrate binding, a conformational change from ES to ES*, which helps position the ptRNA and catalytic metal ions optimally for cleavage, had already been proposed based on results from various kinetic and structural studies (38,39). Because the bacterial RPR's k_{obs} with tight-binding, consensus ptRNAs increases only three fold by the RPP, the possibility of the RPP contributing functional groups to catalysis and thereby increasing k_c (the rate of the chemical step) was discounted. What then accounts for the dramatic RPP-facilitated increase in k_{obs} with non-consensus substrates? Since only K_{conf} and k_c contribute to k_{obs} in a single-turnover trans cleavage reaction, the RPP was then inferred to influence the equilibrium (K_{conf}) that precedes the slower bond-breaking step. By shifting the equilibrium from ES to ES* for the atypical ptRNAs, the bacterial RPP was postulated to stabilize ES* and enhance catalysis (14).

$$\underset{\text{(trans)}}{E + S} \overset{K_D}{\longleftrightarrow} \underset{\text{(cis)}}{ES} \overset{K_{conf}}{\longleftrightarrow} ES^* \xrightarrow{k_c} EP$$

In the case of pt^{Tyr}-S_3-M RPR, the tethered substrate renders it similar to the ES complex in the trans cleavage scheme. *Mja* POP5-RPP30 (but not RPP21-RPP29) enhances k_{obs} for self-cleavage of pt^{Tyr}-S_3-M RPR with a concomitant reduction in the requirement for Mg^{2+}. The k_{obs} for the cis conjugate is dictated only by K_{conf} and k_c. A direct increase in k_c upon addition of *Mja* POP5-RPP30 is unlikely since it would necessitate an alternative mechanism from that employed by the *Mja* RPR, for which there is no evidence. Moreover, both *Mja* and *Eco* RPR cis conjugates exhibit a comparable efficiency suggesting that the functional groups for catalysis are present in the RPR (31). Therefore, the 100-fold increase in k_{obs} upon addition of POP5-RPP30 must arise from increased conversion of ES to ES*. Additional support for this functional parallel between POP5-RPP30 and bacterial RPP stems from the findings that the tertiary structures of archaeal POP5 and bacterial RPP are strikingly similar (40,41), and POP5-RPP30 and *Eco* RPP footprint at similar locations in the C domains of their respective RPRs (16,42–44).

RPP21-RPP29 does not impact the k_{obs} for self-cleavage but probably stabilizes the RPR's tertiary fold and substitutes for some of the RNA–RNA tertiary interactions that strengthen the structural core in bacterial RPRs. In this fashion, it might mirror protein cofactors that facilitate the self-splicing reactions of certain group I introns by tertiary structure capture (36,45; for a comparison of models of the bacterial and archaeal RNase P holoenzymes, see Supplementary Data).

Although RPP21-RPP29 does not contribute to the k_{obs} for self-processing of pt^{Tyr}-S_3-M RPR, it renders pt^{Tyr}-S_3-M RPR active at 100 mM Mg^{2+} (Figure 4A, lanes 2 and 3). The maximal k_{obs} determined for this reaction is similar to that observed for the RPR-alone reaction in the presence of its optimal Mg^{2+} concentration of 500 mM (0.06 versus 0.05 min^{-1}; Table 1). Therefore, RPP21-RPP29 enables the RPR to attain its maximal k_{obs} at a lower Mg^{2+} concentration perhaps by enhancing the affinity of the RNP for Mg^{2+} without affecting ES*. If these RPPs and Mg^{2+} bind to the folded state of the RPR, their binding will be thermodynamically coupled.

Since the *Mja* RPR does not exhibit trans cleavage, we used the rate of self-processing of a cis conjugate as the baseline for its catalytic potential and then determined how RPPs influenced this rate. In the cis construct, the substrate is docked on the enzyme though likely not optimally positioned. If RPP21-RPP29 plays a role in substrate binding, its effect on the catalytic efficiency of a trans cleavage reaction might be more pronounced than in a cis reaction where the substrate is already docked. In fact, RPP21-RPP29 enhances by two fold the k_{obs} for self-cleavage of a cis conjugate with a 5-nt spacer in contrast to a 3-nt-spacer construct where it has no effect (Table 1; data not shown). We are investigating if the pattern of activation by RPPs differs between a cis and a trans cleavage reaction.

The C domain of type M RPR is sufficient for processing a ptRNA provided in cis

Despite the identification of a conserved C domain in all RPRs, previous studies suggested that this domain by itself was either not functional in the absence of cognate RPPs or that its activity was nearly 25 000-fold weaker than the wild type (22,34,35). If this defect is attributable to weak substrate binding, covalent attachment of the substrate should remedy it. Indeed, our study shows that self-cleavage of pt^{Tyr}-S_3-ΔS M RPR is only 12-fold slower than pt^{Tyr}-S_3-M RPR at pH 5.1 (Table 1); moreover, the decreased activity suggests that the S domain does play a role in cleavage even in the cis conjugate (perhaps, by influencing K_{conf}). Such a function of the S domain is clearly redundant with POP5-RPP30 since both pt^{Tyr}-S_3-M RPR and pt^{Tyr}-S_3-ΔS M RPR display near identical rates of self-cleavage in the presence of POP5-RPP30 (Table 1). This result parallels the rescue of the bacterial RPR's C domain by its RPP (35) and once again reveals similarities in the functioning of bacterial and archaeal RNase P.

SUPPLEMENTARY DATA

Supplementary Data are available at NAR Online.

ACKNOWLEDGEMENTS

We are grateful to members of the Gopalan laboratory for useful suggestions and reagents during the course of this investigation, especially to Dr Lien Lai for her advice on cloning strategies and invaluable critique that improved the manuscript. We are indebted to Dr Mark Foster (OSU) for his insightful and important comments on the interpretation of kinetic data. We thank Dr Tim Eubank

(OSU) for generously designing the graphics for Figure 2 in the Supplementary Data, and Drs Edward J. Behrman (OSU), Mark Foster and Roland Hartmann (University of Marburg) for comments on the manuscript. This work was supported by National Institutes of Health Grant R01 GM067807 (to Mark Foster and V.G.) and American Heart Association Pre-Doctoral Fellowship 0515218B (to D.K.P.). Funding to pay the Open Access publication charges for this article was provided in part by private funds and the 2008 US Economic Stimulus payment.

Conflict of interest statement. None declared.

REFERENCES

1. Guerrier-Takada,C., Gardiner,K., Marsh,T., Pace,N.R. and Altman,S. (1983) The RNA moiety of ribonuclease P is the catalytic subunit of the enzyme. *Cell*, **35**, 849–857.
2. Jarrous,N. and Altman,S. (2001) Human ribonuclease P. *Methods Enzymol.*, **342**, 93–100.
3. Hall,T.A. and Brown,J.W. (2002) Archaeal RNase P has multiple protein subunits homologous to eukaryotic nuclear RNase P proteins. *RNA*, **8**, 296–306.
4. Evans,D., Marquez,S.M. and Pace,N.R. (2006) RNase P: interface of the RNA and protein worlds. *Trends Biochem. Sci.*, **31**, 333–341.
5. Gopalan,V. and Altman,S. (2006) The RNA World. In Gesteland,R.F., Cech,T.R. and Atkins,J.F. (eds), CSH Laboratory Press, Cold Spring Harbor, NY, Chapter 6.1 (only online at http://rna.cshl.edu).
6. Walker,S.C. and Engelke,D.R. (2006) Ribonuclease P: the evolution of an ancient RNA enzyme. *Crit. Rev. Biochem. Mol. Biol.*, **41**, 77–102.
7. Pannucci,J.A., Haas,E.S., Hall,T.A., Harris,J.K. and Brown,J.W. (1999) RNase P RNAs from some Archaea are catalytically active. *Proc. Natl Acad. Sci. USA*, **96**, 7803–7808.
8. Harris,J.K., Haas,E.S., Williams,D., Frank,D.N. and Brown,J.W. (2001) New insights into RNase P RNA structure from comparative analysis of the archaeal RNA. *RNA*, **7**, 220–232.
9. Kikovska,E., Svard,S.G. and Kirsebom,L.A. (2007) Eukaryotic RNase P RNA mediates cleavage in the absence of protein. *Proc. Natl Acad. Sci. USA*, **104**, 2062–2067.
10. Brown,J.W. (1999) The ribonuclease P database. *Nucleic Acids Res.*, **27**, 314.
11. Christian,E.L., Zahler,N.H., Kaye,N.M. and Harris,M.E. (2002) Analysis of substrate recognition by the ribonucleoprotein endonuclease RNase P. *Methods*, **28**, 307–322.
12. Hsieh,J., Andrews,A.J. and Fierke,C.A. (2004) Roles of protein subunits in RNA-protein complexes: lessons from ribonuclease P. *Biopolymers*, **73**, 79–89.
13. Kurz,J.C., Niranjanakumari,S. and Fierke,C.A. (1998) Protein component of *Bacillus subtilis* RNase P specifically enhances the affinity for precursor $tRNA^{Asp}$. *Biochemistry*, **37**, 2393–2400.
14. Sun,L., Campbell,F.E., Zahler,N.H. and Harris,M.E. (2006) Evidence that substrate-specific effects of C5 protein lead to uniformity in binding and catalysis by RNase P. *EMBO J.*, **25**, 3998–4007.
15. Sun,L. and Harris,M.E. (2007) Evidence that binding of C5 protein to P RNA enhances ribozyme catalysis by influencing active site metal ion affinity. *RNA*, **13**, 1505–1515.
16. Tsai,H.Y., Pulukkunat,D.K., Woznick,W.K. and Gopalan,V. (2006) Functional reconstitution and characterization of *Pyrococcus furiosus* RNase P. *Proc. Natl Acad. Sci. USA*, **103**, 16147–16152.
17. Li,D., Willkomm,D.K., Schon,A. and Hartmann,R.K. (2007) RNase P of the cyanophora paradoxa cyanelle: A plastid ribozyme. *Biochimie*, **89**, 1528–1538.
18. Pan,T., Loria,A. and Zhong,K. (1995) Probing of tertiary interactions in RNA: 2′-hydroxyl-base contacts between the RNase P RNA and pre-tRNA. *Proc. Natl Acad. Sci. USA*, **92**, 2510–2514.
19. Loria,A. and Pan,T. (1997) Recognition of the T stem-loop of a pre-tRNA substrate by the ribozyme from *Bacillus subtilis* ribonuclease P. *Biochemistry*, **36**, 6317–6325.
20. Oh,B.K. and Pace,N.R. (1994) Interaction of the 3′-end of tRNA with ribonuclease P RNA. *Nucleic Acids Res.*, **22**, 4087–4094.
21. Kirsebom,L.A. and Svard,S.G. (1994) Base pairing between *Escherichia coli* RNase P RNA and its substrate. *EMBO J.*, **13**, 4870–4876.
22. Guerrier-Takada,C. and Altman,S. (1992) Reconstitution of enzymatic activity from fragments of M1 RNA. *Proc. Natl Acad. Sci. USA*, **89**, 1266–1270.
23. Loria,A. and Pan,T. (1996) Domain structure of the ribozyme from eubacterial ribonuclease P. *RNA*, **2**, 551–563.
24. Zahler,N.H., Christian,E.L. and Harris,M.E. (2003) Recognition of the 5′ leader of pre-tRNA substrates by the active site of ribonuclease P. *RNA*, **9**, 734–745.
25. Seif,E., Cadieux,A. and Lang,B.F. (2006) Hybrid *Escherichia coli*-mitochondrial ribonuclease P RNAs are catalytically active. *RNA*, **12**, 1661–1670.
26. Torres-Larios,A., Swinger,K.K., Krasilnikov,A.S., Pan,T. and Mondragon,A. (2005) Crystal structure of the RNA component of bacterial ribonuclease P. *Nature*, **437**, 584–587.
27. Kazantsev,A.V., Krivenko,A.A., Harrington,D.J., Holbrook,S.R., Adams,P.D. and Pace,N.R. (2005) Crystal structure of a bacterial ribonuclease P RNA. *Proc. Natl Acad. Sci. USA*, **102**, 13392–13397.
28. Frank,D.N., Harris,M.E. and Pace,N.R. (1994) Rational design of self-cleaving pre-tRNA-ribonuclease P RNA conjugates. *Biochemistry*, **33**, 10800–10808.
29. Guerrier-Takada,C., Haydock,K., Allen,L. and Altman,S. (1986) Metal ion requirements and other aspects of the reaction catalyzed by M1 RNA, the RNA subunit of ribonuclease P from *Escherichia coli*. *Biochemistry*, **25**, 1509–1515.
30. Smith,D. and Pace,N.R. (1993) Multiple magnesium ions in the ribonuclease P reaction mechanism. *Biochemistry*, **32**, 5273–5281.
31. Kaye,N.M., Christian,E.L. and Harris,M.E. (2002) NAIM and site-specific functional group modification analysis of RNase P RNA: magnesium-dependent structure within the conserved P1-P4 multihelix junction contributes to catalysis. *Biochemistry*, **41**, 4533–4545.
32. Pascual,A. and Vioque,A. (1999) Substrate binding and catalysis by ribonuclease P from cyanobacteria and *Escherichia coli* are affected differently by the 3′ terminal CCA in tRNA precursors. *Proc. Natl Acad. Sci. USA*, **96**, 6672–6677.
33. Andrews,A.J., Hall,T.A. and Brown,J.W. (2001) Characterization of RNase P holoenzymes from *Methanococcus jannaschii* and *Methanothermobacter thermoautotrophicus*. *Biol. Chem.*, **382**, 1171–1177.
34. Green,C.J., Rivera-Leon,R. and Vold,B.S. (1996) The catalytic core of RNase P. *Nucleic Acids Res.*, **24**, 1497–1503.
35. Loria,A. and Pan,T. (1999) The cleavage step of ribonuclease P catalysis is determined by ribozyme-substrate interactions both distal and proximal to the cleavage site. *Biochemistry*, **38**, 8612–8620.
36. Mohr,G., Caprara,M.G., Guo,Q. and Lambowitz,A.M. (1994) A tyrosyl-tRNA synthetase can function similarly to an RNA structure in the *Tetrahymena* ribozyme. *Nature*, **370**, 147–150.
37. Marquez,S.M., Chen,J.L., Evans,D. and Pace,N.R. (2006) Structure and function of eukaryotic ribonuclease P RNA. *Mol. Cell*, **24**, 445–456.
38. Loria,A. and Pan,T. (1998) Recognition of the 5′ leader and the acceptor stem of a pre-tRNA substrate by the ribozyme from *Bacillus subtilis* RNase P. *Biochemistry*, **37**, 10126–10133.
39. Pomeranz Krummel,D.A. and Altman,S. (1999) Multiple binding modes of substrate to the catalytic RNA subunit of RNase P from *Escherichia coli*. *RNA*, **5**, 1021–1033.
40. Kawano,S., Nakashima,T., Kakuta,Y., Tanaka,I. and Kimura,M. (2006) Crystal structure of protein Ph1481p in complex with protein Ph1877p of archaeal RNase P from *Pyrococcus horikoshii* OT3: implication of dimer formation of the holoenzyme. *J. Mol. Biol.*, **357**, 583–591.

41. Wilson,R.C., Bohlen,C.J., Foster,M.P. and Bell,C.E. (2006) Structure of *Pfu* Pop5, an archaeal RNase P protein. *Proc. Natl Acad. Sci. USA*, **103**, 873–878.
42. Tsai,H.Y., Masquida,B., Biswas,R., Westhof,E. and Gopalan,V. (2003) Molecular modeling of the three-dimensional structure of the bacterial RNase P holoenzyme. *J. Mol. Biol.*, **325**, 661–675.
43. Buck,A.H., Kazantsev,A.V., Dalby,A.B. and Pace,N.R. (2005) Structural perspective on the activation of RNase P RNA by protein. *Nat. Struct. Mol. Biol.*, **12**, 958–964.
44. Niranjanakumari,S., Day-Storms,J.J., Ahmed,M., Hsieh,J., Zahler,N.H., Venters,R.A. and Fierke,C.A. (2007) Probing the architecture of the *Bacillus subtilis* RNase P holoenzyme active site by cross-linking and affinity cleavage. *RNA*, **13**, 521–535.
45. Paukstelis,P.J., Chen,J.H., Chase,E., Lambowitz,A.M. and Golden,B.L. (2008) Structure of a tyrosyl-tRNA synthetase splicing factor bound to a group I intron RNA. *Nature*, **451**, 94–97.